Electromagnetic Resonances of Immersed Dielectric Spheres

Chi-Chih Chen, *Member, IEEE*

***Abstract*—The complex natural resonances (CNR) for lossless dielectric spheres in a lossless dielectric medium are investigated. Significant differences between the external and internal resonances are presented. The external resonances are related to the external creeping waves and the internal resonances to the internally reflected waves. The internal resonances are more important in practice because of their smaller damping factors. Simple physical interpretation for predicting the resonance behavior of a general dielectric sphere is obtained.**

***Index Terms*—Electromagnetic scattering, resonance.**

I. Introduction

THE need for a better understanding of dielectric target resonances was found in a study of plastic land-mine classification using the complex natural resonance (CNR) signatures. The CNR's of an immersed dielectric sphere were investigated because of the available exact solutions. Note that the scattering mechanisms of even a simple sphere can be very complicated. Rainbow and glory ray scattering, for example, have been studied for decades [1], [2]. The current paper will focus on the resonant properties of dielectric spheres. Both the sphere and its ambient medium are assumed to be homogeneous, isotropic, and lossless. The CNR's are related to the singularities of expansion coefficients. These CNR's used as a signature are far less damped when the dielectric constant of the sphere exceeds that of the ambient medium. This case will be referred to as a dielectric sphere, whereas the reverse case is designated as a dielectric bubble. The resonances associated with either a dielectric sphere or bubble can be separated into internal and external modes. The internal resonances are caused by the internal waves that experience multiple internal reflections, whereas the external modes are caused by the surface creeping waves. The physical mechanisms associated with the internal and external resonances are explored by examining the resonances of impenetrable spheres and bubbles such as perfect electrical conducting (PEC) and perfect magnetic conducting (PMC) spheres and spherical cavities. The resonance mechanisms of general dielectric spheres or bubbles are highly related to those of impenetrable spheres and bubbles.

Manuscript received September 30, 1997; revised December 12, 1997. This work was supported by the Office of Special Technology (OST) and the Army Research Office's Multi-Disciplinary University Research Initiative (MURI) for humanitarian demining. The opinions or conclusions of this paper do not necessarily represent those of these organizations.

The author is with the ElectroScience Laboratory, The Ohio State University, Columbus, OH 43212 USA.

Publisher Item Identifier S 0018-926X(98)05787-1.

The CNR's of impenetrable cylinders have been examined by numerous authors. These poles are related to surface propagating waves (creeping waves) [3]. The same wave mechanisms are also called "Franz waves" for acoustic scattering from a "rigid sphere" in fluids [4], [5]. This type of wave propagates in the external medium and is mainly determined by the surface geometry instead of the interior material property. Ashkin [6] has shown experimentally that these creeping waves are launched by grazing incident rays. Fahlen and Bryant [7] also provided an astonishing visualization of surface waves on water droplets. Once these creeping waves are launched, they propagate along the surface with attenuation due to the continuous radiation in the tangent direction. The diffraction coefficients of a smooth transparent object has been derived by Chen [8]. Franz and Beckmann [9] also studied the creeping waves for objects of finite conductivity. Chan *et al.* [10] and Barber *et al.* [11] used resonance signatures to characterize dielectric objects. An excellent discussion about the high-frequency scattering by a dielectric sphere is given by Nussenzveig [2], [12]. Although Conwell *et al.* [13] also discussed the resonances of dielectric spheres, they did not separate the internal and external modes. They dealt with only a sphere with refractive index of 1.4. This paper investigates much more general situations and also provides some physical understanding of the resonances associated with dielectric spheres and bubbles. Throughout this chapter, an $(e^{j\omega t})$ time dependence is used.

II. CNR's for Impenetrable Spheres and Bubbles

An impenetrable sphere is defined as a solid PEC or PMC sphere, whereas a impenetrable bubble is a spherical cavity immersed in a infinite PEC or PMC space. The characteristic equations of CNR's for a PEC sphere are written as [14]

$$H^{(2)}_{n+1/2}(k_x a) = 0 \quad (\text{TE}) \qquad \text{and}$$
$$H^{(2)'}_{n+1/2}(k_x a) = 0 \quad (\text{TM}) \tag{1}$$

where "a" is the sphere radius, $H^{(2)}_{n+1/2}$ is the $(n+1/2)_{\text{th}}$ order Hankel function of the second kind, and $k_x = \omega\sqrt{\epsilon_x \mu_x}$, ϵ_x and μ_x are the wavenumber, permittivity, and permeability of the ambient medium. The subscript "x" designates the external medium. The wave whose electrical fields are perpendicular to the radial directions are designated as TE modes. The field components with magnetic fields perpendicular to the radial directions are designated as TM modes. Fig. 1 shows the poles in the complex $k_x a$ space obtained from the above

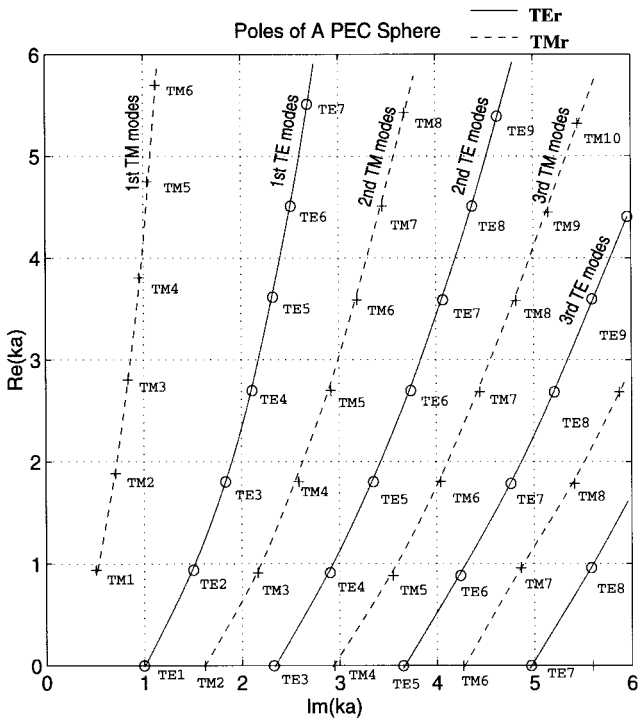

Fig. 1. Normalized complex poles for a PEC sphere. TE and TM poles are marked by "∘" and "+," respectively; the numbers indicate the order.

characteristic equations. The real and imaginary parts of each pole are related to a CNR's resonant frequency and damping factor, respectively. Note that only poles satisfying $\mathrm{Im}(k_x a) \geq 0$ are selected to ensure the damping behavior. A PMC sphere has the same set of characteristic equations as a PEC sphere except that the roll of TM and TE are interchanged. It is well known that the CNR of such impenetrable spheres are caused by the creeping waves as shown by Dragonette and Flax [15]. Since these are impenetrable spheres, the CNR's depend only on the external dielectric constant.

The characteristic equations of CNR's for a PEC bubble are also well known [16] and can be written in terms of Bessel functions and their derivatives such that

$$\begin{aligned} J_{n+1/2}(k_d a) &= 0 \quad (\mathrm{TE}) \qquad \text{and} \\ J'_{n+1/2}(k_d a) &= 0 \quad (\mathrm{TM}) \end{aligned} \tag{2}$$

where $k_d = \omega\sqrt{\epsilon_d \mu_d}$, ϵ_d, and μ_d are the wavenumber, permittivity, and permeability of the internal medium. The subscript "d" designates the internal medium. The roots of the above equations are pure real numbers and the CNR's are pure real, i.e., the resonances are nondamped. This is expected since the cavity is made of PEC. Tables of some the the roots can also be found in [16]. The characteristic equations and the CNR's for PMC bubble can be obtained by simply interchanging the roll of TE and TM. The physical interpretation of resonances inside an impenetrable bubble can be understood by realizing that the Bessel functions represent standing waves formed by incoming and outgoing waves in the radial direction such that

$$J_\lambda(z) = [H_\lambda^{(1)}(z) + H_\lambda^{(2)}(z)]/2 \tag{3}$$

where $\lambda = n + 1/2, z = k_d r$. Using the asymptotic expansion

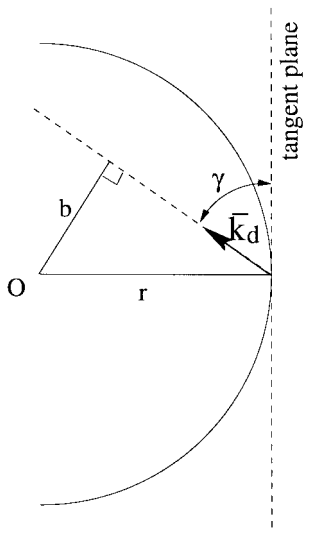

Fig. 2. Internal bounced waves.

for $H_\lambda^{(1)}(z)$ as $z \gg \lambda$ given by [17], one finds

$$\begin{aligned} H_\lambda^{(1)}(z) \sim \sqrt{\frac{2}{\pi^2 z \sin\gamma}} e^{-j(\pi/4)} e^{jz(\sin\gamma - \gamma\cos\gamma)} \\ \cdot \sum_{n=0}^{\infty} A_n \frac{\Gamma\left(n+\frac{1}{2}\right) e^{j(n\pi/2)}}{\left(\frac{z\sin\gamma}{2}\right)^n} \end{aligned} \tag{4}$$

where A_n are coefficients, Γ is the Gamma function, and $\gamma = \cos^{-1}(\lambda/z)$. The factor $e^{jn\pi/2}$ is a result of waves propagating through n caustics. The similar expansion can be readily obtained for $H_\lambda^{(2)}(z)$ by changing the sign of each "j" term. The phase variation in the radial direction is given by the second exponential term. As shown in [18], this phase variation represents an internal wave reflected away from the tangent plane at an angle of γ, as illustrated in Fig. 2.

Similarly, $H_\lambda^{(2)}(k_d r)$ are related to the outgoing portion waves which propagate toward the surface. It is interesting to find that the shortest distance to the sphere center is $b = \lambda/k_d$, for λ mode waves is found to be λ/k_d, which also agrees with the predictions of Nussenzveig [12] using the semiclassical scattering mechanics. In this study, the distance "b" refers to an "impact parameter" associated with the semiclassical collision problem. Also notice that if z increases with λ fixed, then γ increases and b decreases. The suggests that the large argument approximation corresponds to waves propagating closer the radial directions. Under such condition, the roots $j_{\lambda,s}$ and $j'_{\lambda,s}$ associated with (2) can be obtained using the McMahon's expansion [17] for $s \gg \lambda$, such that

$$\begin{aligned} j_{n+(1/2),s} &\sim \pi\left(\frac{n}{2} + s\right) \quad \text{and} \\ j'_{n+(1/2),s} &\sim \pi\left(\frac{n-1}{2} + s\right). \end{aligned} \tag{5}$$

Thus, the corresponding resonant frequencies are

$$\begin{aligned} f_{n,s}^{\mathrm{TE}} &\sim \frac{v_d}{2a}\left(\frac{n}{2} + s\right) \quad \text{and} \\ f_{n,s}^{\mathrm{TM}} &\sim \frac{v_d}{2a}\left(\frac{n-1}{2} + s\right) \end{aligned} \tag{6}$$

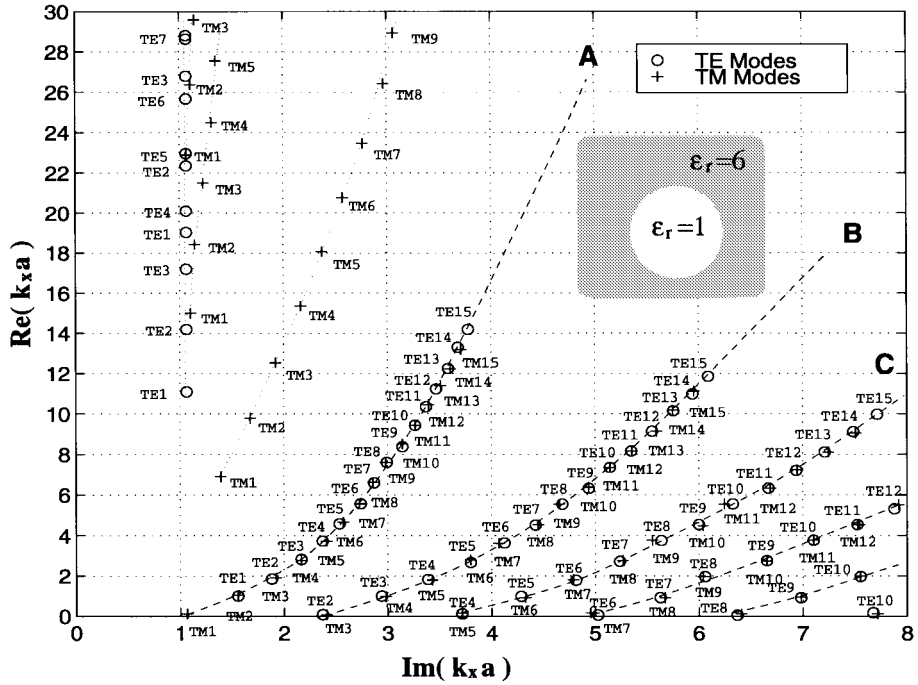

Fig. 3. Normalized poles for a dielectric bubble.

where v_d is the internal plane wave phase velocity. These resonant frequencies are the same as those found in a confocal case Fabry–Perot resonator [19].

III. CNR's For General Dielectric Bubbles

The characteristic equations of the CNR's for general dielectric spheres can be obtained from the denominators of the expansion coefficients in the normal mode-field expansions given by Harrington [20]. They are

$$\sqrt{\epsilon_d\mu_x}\hat{H}_n^{(2)}(k_xa)\hat{J}_n'(k_da) - \sqrt{\epsilon_x\mu_d}\hat{H}_n^{(2)'}(k_xa)\hat{J}_n(k_da) = 0, \quad \text{(TE)} \quad \text{and} \tag{7}$$

$$\sqrt{\epsilon_x\mu_d}\hat{H}_n^{(2)}(k_xa)\hat{J}_n'(k_da) - \sqrt{\epsilon_d\mu_x}\hat{H}_n^{(2)'}(k_xa)\hat{J}_n(k_da) = 0, \quad \text{(TM)} \tag{8}$$

where $\hat{J}_n$ and $\hat{H}_n$ are nth order modified spherical Bessel and Hankel functions. In this paper, it is assumed that $\mu_x = \mu_d = \mu_0$ (free-space permeability).

The CNR behavior for a dielectric bubble whose internal permittivity is less than that of the ambient medium is now studied. The poles in ka-space can be found from (7) nad (8). As an example, we consider $\epsilon_d = \epsilon_0, \epsilon_x = 6\epsilon_0$ and $\mu_d = \mu_x = \mu_0$. The corresponding poles are plotted in Fig. 3, where TE- and TM-mode pole are marked by "$\circ$" and "$+$," respectively. This figure is currently plotted in the k_xa space, i.e., it is normalized by the external medium. Later, the poles will be revisited in the k_da space to study the internal resonant modes. Two different groups of poles can be clearly distinguished by their different vertical separation between adjacent modes. The first group of poles which have smaller vertical separations are linked by dashed lines, A, B, C, $\cdots$, etc. Each line corresponds to the multiple poles associated with an order number n. The second group of poles which have larger vertical separations are linked by dotted lines. Each group will be examined separately.

A. External Resonances

Let us focus on the first group of poles (on lines A, B, $\cdots$, etc.) and compare them with the poles for a PMC sphere immersed in the same medium as shown in Fig. 4. The TE and TM poles for the PMC sphere are marked by "$\times$" and "$*$," respectively. It is observed that the TM_n poles for the current dielectric bubble (marked by "$+$") are located very close to the TM_n mode poles (marked by "$\times$") for the PMC sphere and that the TE_n mode poles are located close to TM_{n+1} mode poles for the PMC sphere [18]. If one allows $\epsilon_x \to \infty$ but with $\sqrt{\epsilon_x\mu_x}$ fixed, the ambient becomes PMC and, thus, the TE_n mode poles of the dielectric bubble will approach to the TE_n mode poles of a PMC sphere.

From the above comparison, it is obvious that the CNR's of this group are external resonances and similar to those found for the an impenetrable sphere. Since these CNR's are caused by the surface creeping waves and are mainly determined by the geometry and the property of the ambient medium they are fairly insensitive to the internal property. This is clearly demonstrated in Fig. 5 where the CNR's for bubbles with internal dielectric constants of 1 and 2 are compared. As one can see, both cases have similar external CNR's locations.

B. Internal Resonances

Now the behavior of the second group of CNR's found in Fig. 3 will be examined by replotting the poles in the k_d space as shown in Fig. 6. Notice that most external poles are not included here. Three major features are observed from this group of CNR's are: 1) all the poles have imaginary parts greater than 4.3 indicating a low bound of damping factors;

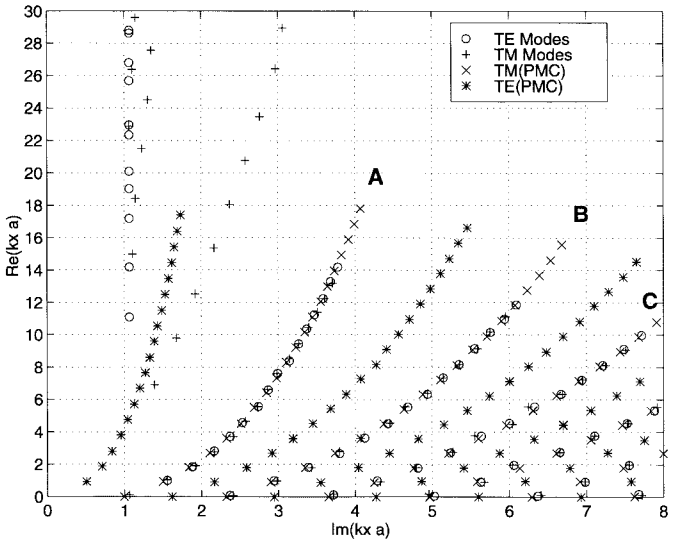

Fig. 4. Pole comparison for dielectric bubbles and for PMC spheres.

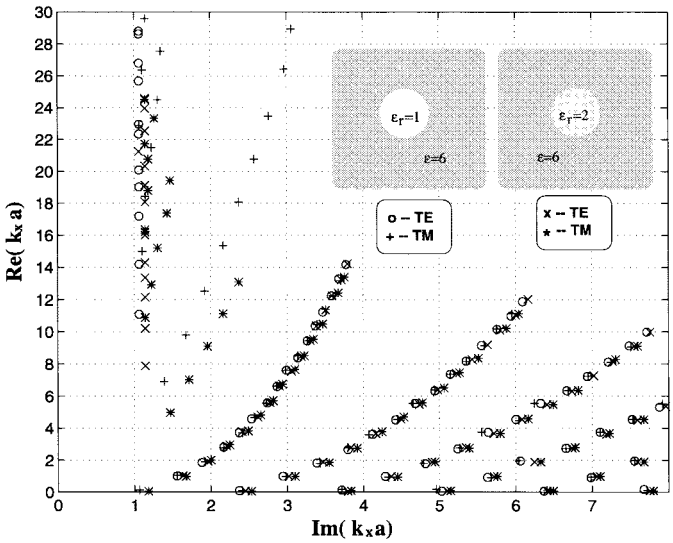

Fig. 5. Comparison of surface wave poles for dielectric bubbles with different internal permittivity.

2) smaller imaginary parts compared to most external poles studied earlier suggest lower damped resonances and more practical use; 3) TE-mode poles have smaller imaginary parts than those of TM-mode poles. In fact, all TE-mode poles tends to have the same imaginary parts. Further discussion of this behavior is explored below.

Physically, a dielectric bubble and a PEC spherical cavity of the same size and internal material are similar as far as the internal resonances are concerned. However, the former experiences damping due to energy leakage through the penetrable surface and the latter is undamped. The resonant frequency is determined by the coherent condition including the propagation phase, the phase of surface reflection at each bounce and the phase jumps due to caustics. Since all these properties are the same between a dielectric bubble and a PEC spherical cavity, one would expect them to have a very similar resonant spectrum. This prediction is verified by comparing their resonant frequencies of the first two modes $(s = 1, 2)$ for the lowest five orders $(n = 1, \cdots, 5)$, as shown in Table I. Indeed, very similar resonant frequencies are observed for both cases. This indicates that this group of CNR's shares the same resonant mechanism as were previously found for a spherical PEC cavity. This important discovery suggests that these CNR's are internal type and are insensitive to the external medium.

The damping factors for a spherical PEC cavity and a dielectric bubble are completely different. The CNR's for the PEC cavity are nondamped, however, the CNR's for a dielectric bubble are damped due to the energy leakage through the partial transmission process occurring at each internal reflection. In order to understand their damping behavior, the spherical interface is locally approximated by a plane interface near the reflection points. At each internal reflection, partial energy leaks out the sphere through the transmission process and the magnitude of the remained wave decreases according to the reflection coefficient, which is determined by the incident angle, the polarization, and the internal/external dielectric contrast. Assume that a particular internal resonant mode is formed by a plane wave experiencing M internal reflections as illustrated in Fig. 7. It is easy to show that the time period T is $M(2a\cos\theta_i)/v_d$, where a is the radius, θ_i is the incident angle, and $v_d = 1/\sqrt{\epsilon_d \mu_d}$ is the internal phase velocity. Define an *effective damping factor* (EDF) α_e and the *normalized effective damping factor* (NEDF) χ as

$$e^{-\alpha_e T} \equiv |R|^M \quad \text{i.e.}$$
$$\alpha_e \equiv -\frac{v_d}{2a\cos\theta_i}\ln|R| \quad \text{and} \tag{9}$$
$$\chi \equiv \frac{a}{v_d}\alpha_e = -\frac{1}{2\cos\theta_i}\ln|R|. \tag{10}$$

The reflection coefficient R is defined as

$$R^{\mathrm{TE}} = \frac{Z_x/\cos\theta_t - Z_d/\cos\theta_i}{Z_x/\cos\theta_t + Z_d/\cos\theta_i}, \quad \text{or}$$
$$R^{\mathrm{TM}} = \frac{Z_x\cos\theta_t - Z_d\cos\theta_i}{Z_x\cos\theta_t + Z_d\cos\theta_i} \tag{11}$$

where $Z_x = \sqrt{\mu_x/\epsilon_x}$, $Z_d = \sqrt{\mu_d/\epsilon_d}$, and θ_t is the refraction angle.

The NEDF for the current bubble case whose internal and external dielectric constants are one and six, respectively, is shown in Fig. 8. Note that χ for both TE and TM mode are always larger than 0.43 which corresponds to waves bounced back and forth along the radial direction, similar to a "Fabry–Perot resonator." Note that TE modes have much smaller damping than TM modes. The behavior of the NEDF predicts correctly the imaginary parts of the actual CNR's observed in Fig. 6. The damping behavior of the internal CNR's of a dielectric bubble can be predicted by a simple model involving multiple reflections. As the dielectric contrast increases, the amplitude of the reflection coefficient also increases. The resonance becomes less damped.

IV. CNR's For General Dielectric Spheres

The CNR behavior for general dielectric spheres is now investigated by considering the internal and external resonances

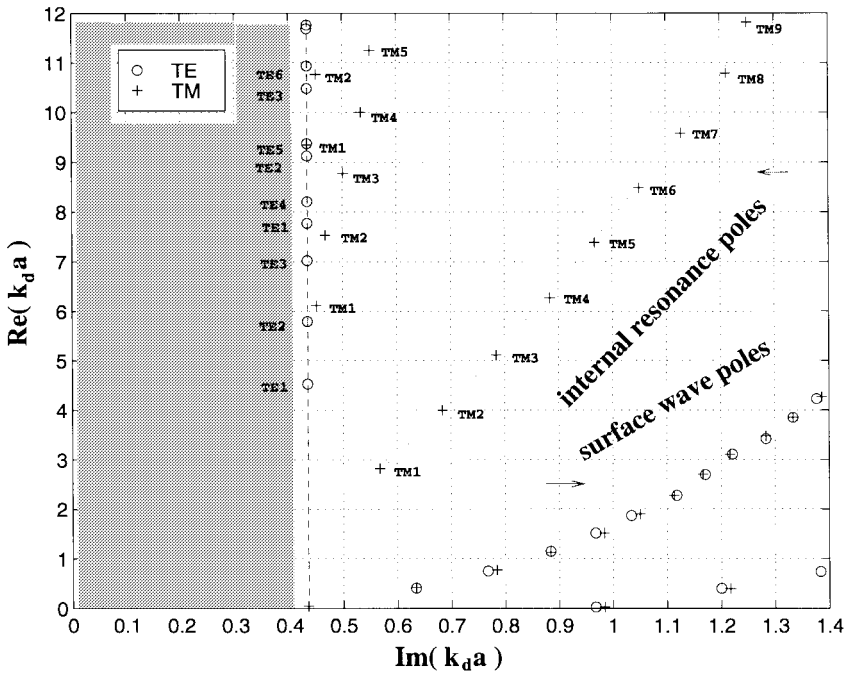

Fig. 6. Normalized poles ($k_d a$ space) for a dielectric bubble.

TABLE I
COMPARING THE NORMALIZED RESONANT FREQUENCIES $\mathrm{Re}(k_d a)$ OF THE FIRST AND SECOND MODES ($s = 1, 2$) POLES ($n = 1, \cdots, 5$) FOR A DIELECTRIC BUBBLE WITH THOSE FOR A PEC BUBBLE

$k_d a$	Dielectric Bubble				PEC Spherical Cavity			
n	$TE_{n,1}$	$TE_{n,2}$	$TM_{n,1}$	$TM_{n,2}$	$TE_{n,1}$	$TE_{n,2}$	$TM_{n,1}$	$TM_{n,2}$
1	4.52	7.77	2.81	6.12	4.49	7.73	2.74	6.12
2	5.80	9.13	4.00	7.51	5.76	9.10	3.87	7.44
3	7.02	10.48	5.12	8.77	6.99	10.42	4.97	8.72
4	8.20	11.68	6.28	9.98	8.18	11.71	6.06	9.97
5	9.38	12.99	7.38	11.24	9.36	12.97	7.14	11.19

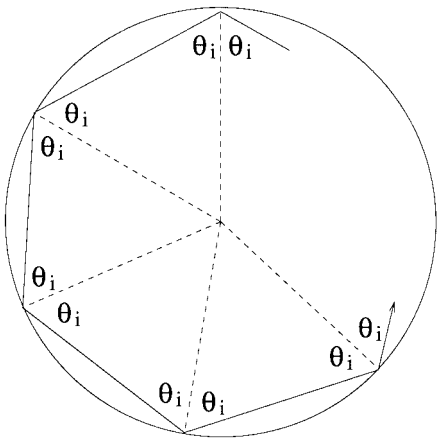

Fig. 7. An internal wave going through multiple internal reflections.

separately. Let us first examine the CNR's for a dielectric sphere ($\epsilon_r = 9$) in free-space, as shown in Fig. 9. The poles are plotted in $k_d a$ space to focus on the internal CNR's.

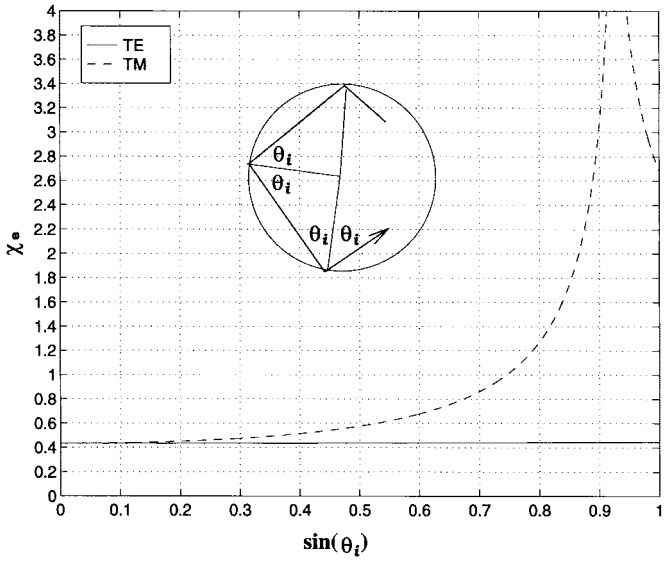

Fig. 8. Normalized effective damping factors (NEDF's) χ for dielectric bubble with internal and external dielectric being one and six, respectively.

Only a few of the external CNR's are visible as indicated by "surface wave poles." These CNR's show quite different behavior compared to those for the bubbles.

A. Internal Resonances

Several noticeable features are observed from Fig. 7. Both TE and TM modes can have very small imaginary parts and, thus, small damping. This is very important for practical applications. Second, all internal TE-mode CNR's are located to the left of a certain vertical line $\mathrm{Im}(k_d a) \approx 0.38$. Third, the imaginary parts of all internal TM-mode CNR's increase first as their order numbers increase and then decrease after

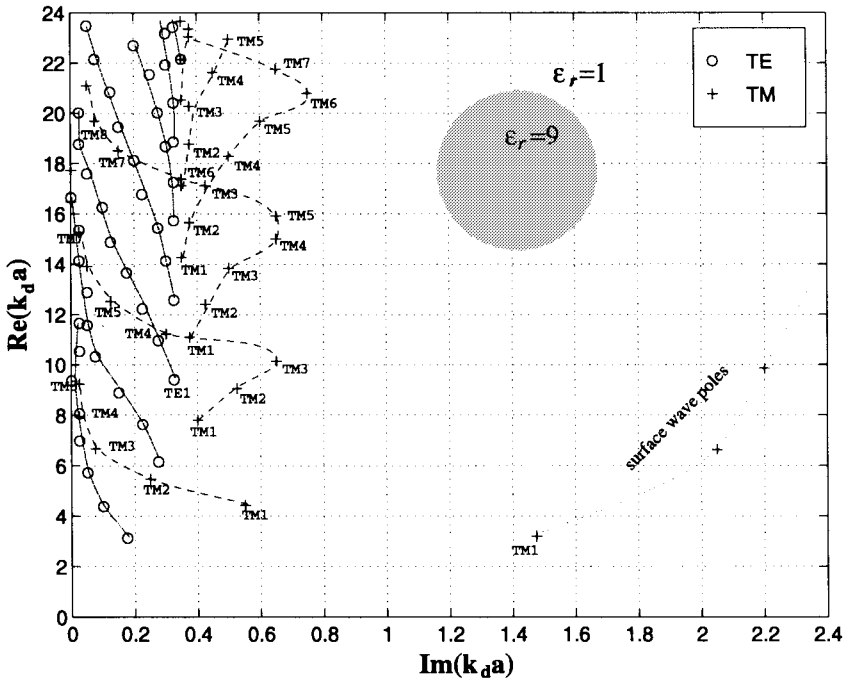

Fig. 9. Normalized poles for a dielectric sphere ($\epsilon_r = 9$) in free-space.

TABLE II
COMPARING THE NORMALIZED RESONANT FREQUENCIES $Re(d_d a)$ OF THE FIRST MODE ($s = 1$) POLES OF ORDER $n = 1, \cdots, 5$, FOR A DIELECTRIC SPHERE ($\epsilon_r = 9$) WITH THOSE FOR A PMC SPHERICAL CAVITY

$k_d a$	Dielectric Sphere				PMC bubble			
n	$TM_{n,1}$	$TM_{n,2}$	$TE_{n,1}$	$TE_{n,2}$	$TM_{n,1}$	$TM_{n,2}$	$TE_{n,1}$	$TE_{n,2}$
1	4.37	7.75	3.05	6.18	4.49	7.73	2.74	6.12
2	5.32	9.08	4.37	7.60	5.76	9.10	3.87	7.44
3	6.71	10.15	5.69	8.90	6.99	10.42	4.97	8.72
4	8.03	11.23	6.95	10.31	8.18	11.71	6.06	9.97
5	9.23	12.52	8.09	11.57	9.36	12.97	7.14	11.19

a certain order of numbers. The lowest branch TM modes become less damped after the very first pole. All these features will be examined below.

It was shown that the resonant frequencies inside a dielectric bubble are very close to those inside a PEC spherical cavity (see Tables I) since both have similar geometrical properties except that the dielectric bubble has a penetrable boundary, which results in damped resonances. Similarly, one would expect the internal resonant frequencies for a dielectric sphere to be close to those for a PMC spherical cavity. This prediction is immediately verified by the close agreement when comparing the resonant frequencies of the first two modes ($s = 1, 2$) for the five lowest orders ($n = 1, \cdots, 5$), as shown in Table II. The internal dielectric constant for both cases is equal to nine. Therefore, the internal CNR's for a dielectric sphere are caused by the same internal reflection mechanism as a in dielectric-filled PMC bubble.

It was shown that the internal CNR damping behavior associated with a dielectric bubble can be predicted from normalized effective damping factor (NEDF). Its damping was due to the partially reflected waves. Here, the NEDF is used again to predict the internal CNR damping behavior associated with a dielectric sphere. The new NEDF plot is shown in Fig. 10.

Total reflections occurs when the incident angle θ_i is greater than the critical angle θ_c, where $\sin\theta_c = 1/\sqrt{9} \approx 0.33$. It is also noticed that for TM mode, a zero reflection occurs at the Brewster angle θ_B where $\sin\theta_B = 0.3163$. It is also noticed that χ for the TE modes are always smaller than 0.35 and decrease as $\sin\theta_i$ increases until θ_i reaches the critical angle θ_c. Beyond the critical angle χ becomes zero and the CNR becomes undamped. For the TM mode, χ first increases from 0.35 as θ_i increases in the $\theta_i < \theta_B$ region. In $\theta_B < \theta_i < \theta_c$ region, χ decreases to zero again and remains to be zero for $\theta_i > \theta_c$. It is intriguing to notice that this unique TM mode "turning back" behavior agrees with what observed in Fig. 6. Further investigation about the turning point using the previous relation $\sin\theta_i \approx (n + 1/2/\mathrm{Re}(k_d a))$ with $\mathrm{Im}(k_d a)$ much less than $\mathrm{Re}(k_d a))$ shows that the turning points occur when $\theta_i \approx \theta_B$.

B. Internal and External CNR Coupling

In Fig. 9, the internal and external CNR's for dielectric sphere ($\epsilon_r = 9$) in free-space are well separated due to the very different imaginary part (or damping factor). As the dielectric difference between the sphere and the ambient medium decreases, the internal reflection coefficient decrease and, thus, the damping increases. This will move the internal CNR's closer to the external CNR's. Figs. 11 and 12 plot the CNR's for dielectric spheres whose dielectric constants are six and three, respectively. Comparing these with Fig. 9, one can clearly see that the internal CNR's become more damped.

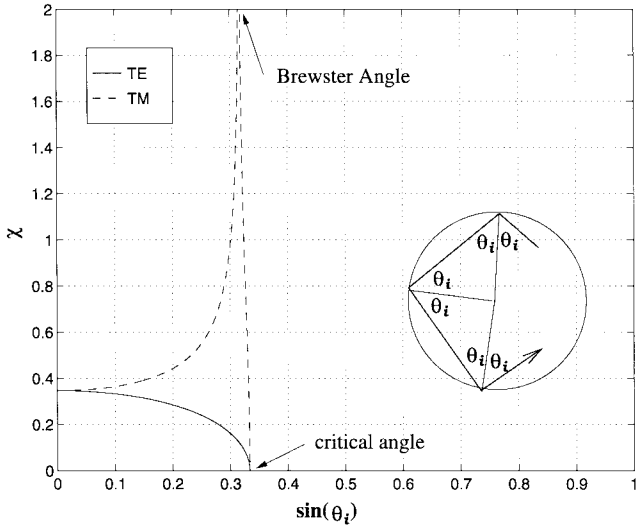

Fig. 10. Normalized effective damping factor (NEDF) χ for dielectric sphere with internal and external dielectric constant being nine and one, respectively.

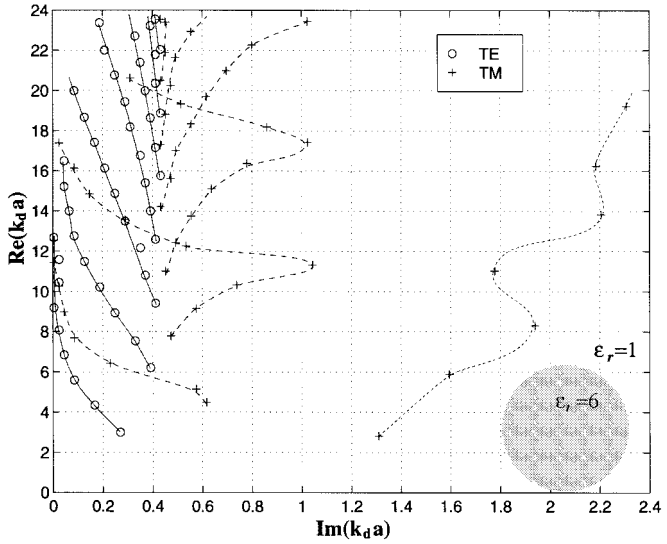

Fig. 11. Normalized poles for a dielectric sphere $(\epsilon_r = 6)$ in free-space.

Fig. 11 shows that some external pole locations belonging to the left-most string have been affected. This results in an unusual properties of this string. Much stronger coupling is also seen in Fig. 12 where the behavior of the first string of external CNR's have been completely altered as shown by the dotted line. The vertical spacing of this string is no longer the same as would be expected from a purely external resonances. The spacing of the high-order poles becomes similar to that of internal resonances. Strictly speaking, one can no longer classify them as either internal or external resonances.

C. External Resonances

It has been shown that the resonant frequencies and damping factors of external modes for a dielectric bubble are very similar to those for an impenetrable PMC sphere due to the similar surface wave mechanism caused by the continuous curvature diffraction. It was also shown that those external modes are insensitive to the internal medium. Similar properties will be shown to exist for the external resonances associated with a dielectric sphere except that the PMC sphere is replaced by a PEC sphere and the damping factors of the TE modes are more sensitive to the internal medium. Fig. 13 plots the poles for a dielectric sphere $(\epsilon_r = 9)$ in free-space in the $k_x a$ space. The TE- and TM-mode poles are marked by "$\circ$" and "$+$," respectively. For comparison, the normalized TE and TM poles associated with a PEC sphere are also plotted and marked by "$\times$" and "$*$," respectively. The following discussion focuses on the external resonant poles indicated by the strings marked by $A, B, C, \cdots$, etc. As one can see, the TM poles are located very close to those for a PEC sphere except for string A whose locations are affected by the internal resonance poles, as discussed earlier. It is also observed that all the external TE-mode poles deviate from the PEC poles toward higher damping factors (i.e., right of the figure). Nevertheless, all TE-mode resonant frequencies remain close to those associated with a PEC sphere whose resonant frequencies are determined by the phase velocities of the surface creeping waves and independent of internal material. Therefore, it is concluded that the external resonances of a dielectric sphere are caused by creeping waves similar to those on a PEC sphere except that the former have larger damping factors. For impenetrable spheres, the damping is due to the continuous power lost by radiating waves away from the spherical surface along the tangent direction. For a dielectric sphere, in addition to the radiation tangent to the surface, part of energy is continuously shedding into the sphere at the critical angle direction. The existence of such a wave mechanism was first suggested by van der Hulst [21] while studying the resonant peaks observed in the scattered fields from rain droplets. This unique process does not occur in the dielectric bubble case since no internal critical angle exists.

As the dielectric contrast decreases, the A-string pole locations become severely distorted as the internal CNR poles move further away from the real axis as discussed earlier. This is demonstrated by Fig. 14. All other surface wave poles also move farther away from the PEC poles to the right, as shown in Fig. 14.

V. Summary and Conclusion

The main contribution of this study is to provide a simple physical interpretation for predicting the resonance behavior of a general dielectric sphere. This is achieved by: 1) interpreting the internal standing waves as internal bouncing waves whose incident angles upon the sphere boundary are determined by $k_d a$ and n; 2) relating the internal and external resonances to those for impenetrable cavities and spheres, respectively; and 3) using a simple flat interface reflection/transmission model and the newly defined effective damping factor (EDF) to correctly predict the damping behavior of the internal resonances.

The resonances of a dielectric sphere (or bubble) were separated into external modes and internal modes. The former are caused by the surface creeping waves and have been shown to be very similar to PEC (or PMC) spheres. These external

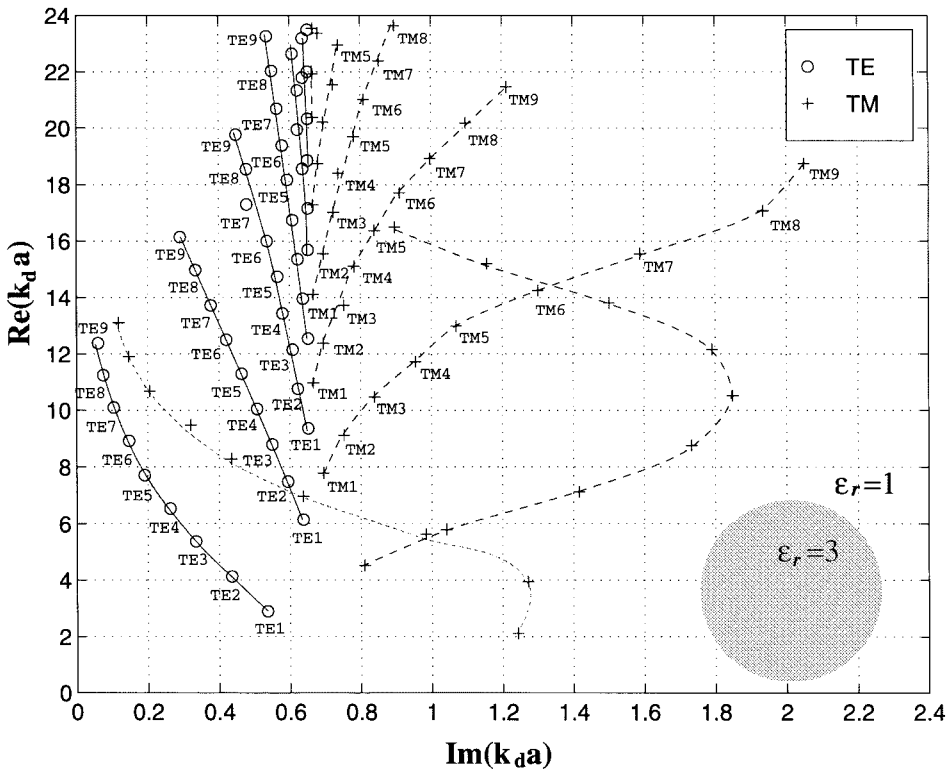

Fig. 12. Normalized poles for a dielectric sphere ($\epsilon_r = 3$) in free-space.

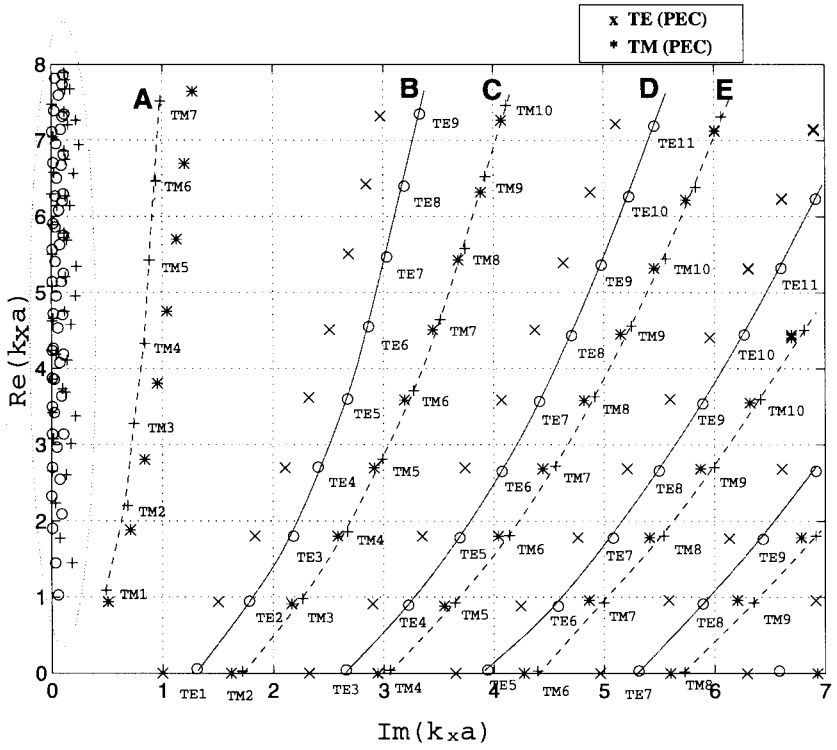

Fig. 13. Normalized poles in the $k_x a$ space for a dielectric sphere ($\epsilon_d = 9\epsilon_0$) in free-space. ($\circ$) TE modes ($+$) TM modes (x) TE modes for PEC sphere ($*$) TM modes for PEC sphere.

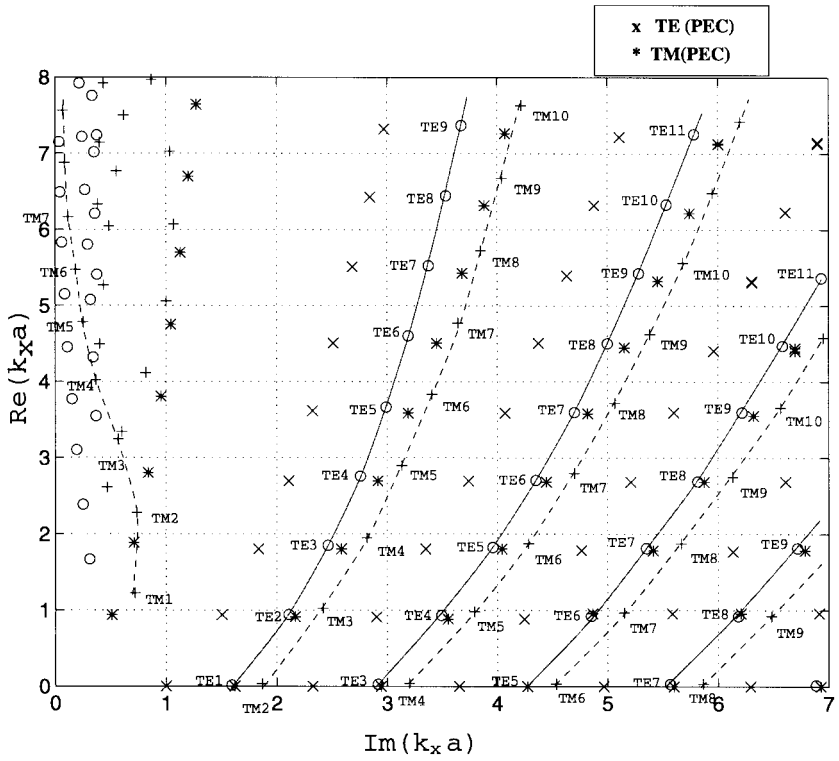

Fig. 14. Normalized poles for a dielectric sphere ($\epsilon_d = 3\epsilon_0$) in free-space. ($\circ$) TE modes ($+$) TM modes (x) TE modes for PEC sphere ($*$) TM modes for PEC sphere.

resonances are fairly independent of internal material. They are also found to have much larger damping factors compared to the internal resonances and, thus, are less important in practice. The internal resonances associated with a dielectric sphere (or bubble) were shown to be related to internal bouncing waves which experience multiple reflections. Their resonant frequencies were shown to be close to those of an impenetrable PMC (or PEC) bubble filled with the same dielectric material. It was also found that the internal resonances associated with a dielectric bubble are mainly in the radial direction. The damping of internal resonances is determined by the amount of energy transmitted out at each internal reflection. For both dielectric sphere and bubble, it was found that the internal TE modes are usually less damped than the TM modes. For dielectric spheres, it is interesting to find that higher TM modes could have very small damping factors when the internal incident angle is larger than the Brewster angle. A final note here is that almost all external resonance poles and off-axis internal resonance poles do not satisfy the large argument approximation, i.e., $ka \gg n$. Therefore, they are often not included in the literature that studies the resonances using large argument approximations.

From this study, it was found that the internal CNR's are less damped than the external ones. It was also found that the internal CNR's for a dielectric sphere are much less damped than those for a dielectric bubble. Therefore, it would be expected that the CNR's for buried plastic land mines would correspond to the bubble case and would be highly damped.

ACKNOWLEDGMENT

The author would like to thank Dr. L. Peters, Jr. for motivating this study and for his helpful discussions.

REFERENCES

[1] L. Peters and W. G. Swarner, "Approximations for dielectric or plasma scatters," *Proc. IEEE*, vol. 53, pp. 882–892, Aug. 1965.
[2] H. M. Nussenzveig, "High-frequency scattering by a transparent sphere—Part I: Direct reflection and transmission; Part II: Theory of the rainbow and the glory," *J. Math. Phys.*, vol. 10, pp. 82–177, Jan. 1969.
[3] W. Franz, "Uber die Greenschen funktionen des zylinders und der kugel," *Z. Naturforsch.*, vol. A-9, pp. 705–716, 1954.
[4] G. V. Frisk, J. W. Dickey, and H. Überall, "Surface wave modes on elastic cylinders," *J. Acoust. Soc. Amer.*, vol. 58, pp. 996–1008, Nov. 1975.
[5] G. V. Frisk and H. Überall, "Creeping waves and lateral waves in acoustic scattering by large elastic cylinders," *J. Acoust. Soc. Amer.*, vol. 59, pp. 46–53, Jan. 1976.
[6] A. Ashkin and J. M. Dziedzic, "Observation of optical resonances of dielectric spheres by light scattering," *J. Appl. Optics*, vol. 20, pp. 1803–1814, May 1981.
[7] T. S. Fahlen and H. C. Bryant, "Direct observation of surface waves on water droplets," *J. Optical Soc. Amer.*, vol. 56, pp. 1635–1636, Nov. 1966.
[8] Y. M. Chen, "Diffraction by a smooth transparent object," *J. Math. Phys.*, vol. 5, pp. 820–832, June 1964.
[9] W. Franz and P. Beckmann, "Creeping waves for objects of finite conductivity," *IRE Trans. Antennas Propagat.*, vol. AP-4, pp. 203–208, 1956.
[10] L. C. Chan, D. L. Moffatt, and L. Peters, "A characterization of subsurface radar targets," *Proc. IEEE*, vol. 67, pp. 991–1000, July 1979.
[11] P. Barber, J. F. Owen, and R. K. Chang, "Resonant scattering for characterization of axisymmetric dielectric objects," *IEEE Trans. Antennas Propagat.*, vol. AP-30, pp. 168–172, Mar. 1982.
[12] H. M. Nussenzveig, *Diffraction Effects in Semiclassical Scattering*. Cambridge, U.K.: Cambridge Univ. Press, 1992.

[13] P. R. Conwell, P. W. Barber, and C. K. Rushforth, "Resonant spectra of dielectric spheres," *J. Acoust. Soc. Amer.*, vol. 1, pp. 62–67, Jan. 1984.
[14] R. F. Harrington, *Time-harmonic Electromagnetic Fields*. New York: McGraw-Hill, 1961, p. 294.
[15] L. R. Dragonette and L. Flax, "Relation between creeping waves and normal modes of vibration of a curved body," *J. Acoust. Soc. Amer.*, vol. 61, pp. 711–715, Mar. 1977.
[16] R. F. Harrington, *Time-harmonic Electromagnetic Fields*. New York: McGraw-Hill, 1961, pp. 269–270.
[17] M. Abramowitz and I. A. Stegun, *Handbook of Mathematical Functions*. New York: Dover, 1972.
[18] C.-C. Chen, "Design and development of ground penetrating radar systems for the detection and classification of unexploded ordnances and land mines," Ph.D. dissertation, Ohio State Univ., Columbus, Aug. 1997.
[19] H. A. Haus, *Waves and Fields in Optoelectronics*. Englewood Cliffs, NJ: Prentice-Hall, 1984, p. 127.
[20] R. F. Harrington, *Time-harmonic Electromagnetic Fields*. New York: McGraw-Hill, 1961, pp. 292–298.
[21] H. C. van de Hulst, *Light Scattering by Small Particles*. New York: Wiley, 1957.

Chi-Chih Chen (M'92) was born in Taiwan, R.O.C. He received the B.E.E. degree from the National Taiwan University, in 1988, and the M.Sc. and Ph.D. degrees in electrical engineering from The Ohio State University, Columbus, in 1993 and 1997, respectively.

In 1992 he became a Graduate Research Associate in the ElectroScience Laboratory, Department of Electrical Engineering, The Ohio State University, where he is now a Postdoctoral Researcher. His primary interests are in the fields of antenna design, signal processing, and radar measurements. He is currently involved in ground-penetrating radar applications for detecting and classifying unexploded ordnance and antipersonnel mines.

Dr. Chen is a member of Sigma Xi and Phi Kappa Phi honor societies.